Properties of Jets in W Boson Events from 1.8 TeV $\overline{p}p$ Collisions

F. Abe,[17] H. Akimoto,[38] A. Akopian,[31] M. G. Albrow,[7] S. R. Amendolia,[27] D. Amidei,[20] J. Antos,[33] S. Aota,[36] G. Apollinari,[31] T. Arisawa,[38] T. Asakawa,[36] W. Ashmanskas,[18] M. Atac,[7] F. Azfar,[26] P. Azzi-Bacchetta,[25] N. Bacchetta,[25] W. Badgett,[20] S. Bagdasarov,[31] M. W. Bailey,[22] J. Bao,[40] P. de Barbaro,[30] A. Barbaro-Galtieri,[18] V. E. Barnes,[29] B. A. Barnett,[15] M. Barone,[9] E. Barzi,[9] G. Bauer,[19] T. Baumann,[11] F. Bedeschi,[27] S. Behrends,[3] S. Belforte,[27] G. Bellettini,[27] J. Bellinger,[39] D. Benjamin,[35] J. Benlloch,[19] J. Bensinger,[3] D. Benton,[26] A. Beretvas,[7] J. P. Berge,[7] J. Berryhill,[5] S. Bertolucci,[9] S. Bettelli,[27] B. Bevensee,[26] A. Bhatti,[31] K. Biery,[7] M. Binkley,[7] D. Bisello,[25] R. E. Blair,[1] C. Blocker,[3] S. Blusk,[30] A. Bodek,[30] W. Bokhari,[26] G. Bolla,[29] V. Bolognesi,[2] Y. Bonushkin,[4] D. Bortoletto,[29] J. Boudreau,[28] L. Breccia,[2] C. Bromberg,[21] N. Bruner,[22] E. Buckley-Geer,[7] H. S. Budd,[30] K. Burkett,[20] G. Busetto,[25] A. Byon-Wagner,[7] K. L. Byrum,[1] C. Campagnari,[7] M. Campbell,[20] A. Caner,[27] W. Carithers,[18] D. Carlsmith,[39] J. Cassada,[30] A. Castro,[25] D. Cauz,[27] Y. Cen,[30] A. Cerri,[27] F. Cervelli,[27] P. S. Chang,[33] P. T. Chang,[33] H. Y. Chao,[33] J. Chapman,[20] M. -T. Cheng,[33] M. Chertok,[34] G. Chiarelli,[27] T. Chikamatsu,[36] C. N. Chiou,[33] L. Christofek,[13] S. Cihangir,[7] A. G. Clark,[10] M. Cobal,[27] E. Cocca,[27] M. Contreras,[5] J. Conway,[32] J. Cooper,[7] M. Cordelli,[9] C. Couyoumtzelis,[10] D. Crane,[1] D. Cronin-Hennessy,[6] R. Culbertson,[5] T. Daniels,[19] F. DeJongh,[7] S. Delchamps,[7] S. Dell'Agnello,[27] M. Dell'Orso,[27] R. Demina,[7] L. Demortier,[31] M. Deninno,[2] P. F. Derwent,[7] T. Devlin,[32] J. R. Dittmann,[6] S. Donati,[27] J. Done,[34] T. Dorigo,[25] A. Dunn,[20] N. Eddy,[20] K. Einsweiler,[18] J. E. Elias,[7] R. Ely,[18] E. Engels, Jr.,[28] D. Errede,[13] S. Errede,[13] Q. Fan,[30] G. Feild,[40] Z. Feng,[15] C. Ferretti,[27] I. Fiori,[2] B. Flaugher,[7] G. W. Foster,[7] M. Franklin,[11] M. Frautschi,[35] J. Freeman,[7] J. Friedman,[19] H. Frisch,[5] Y. Fukui,[17] S. Funaki,[36] S. Galeotti,[27] M. Gallinaro,[26] O. Ganel,[35] M. Garcia-Sciveres,[18] A. F. Garfinkel,[29] C. Gay,[11] S. Geer,[7] D. W. Gerdes,[15] P. Giannetti,[27] N. Giokaris,[31] P. Giromini,[9] G. Giusti,[27] L. Gladney,[26] M. Gold,[22] J. Gonzalez,[26] A. Gordon,[11] A. T. Goshaw,[6] Y. Gotra,[25] K. Goulianos,[31] H. Grassmann,[27] L. Groer,[32] C. Grosso-Pilcher,[5] G. Guillian,[20] J. Guimarães,[15] R. S. Guo,[33] C. Haber,[18] E. Hafen,[19] S. R. Hahn,[7] R. Hamilton,[11] R. Handler,[39] R. M. Hans,[40] F. Happacher,[9] K. Hara,[36] A. D. Hardman,[29] B. Harral,[26] R. M. Harris,[7] S. A. Hauger,[6] J. Hauser,[4] C. Hawk,[32] E. Hayashi,[36] J. Heinrich,[26] B. Hinrichsen,[14] K. D. Hoffman,[29] M. Hohlmann,[5] C. Holck,[26] R. Hollebeek,[26] L. Holloway,[13] S. Hong,[20] G. Houk,[26] P. Hu,[28] B. T. Huffman,[28] R. Hughes,[23] J. Huston,[21] J. Huth,[11] J. Hylen,[7] H. Ikeda,[36] M. Incagli,[27] J. Incandela,[7] G. Introzzi,[27] J. Iwai,[38] Y. Iwata,[12] H. Jensen,[7] U. Joshi,[7] R. W. Kadel,[18] E. Kajfasz,[25] H. Kambara,[10] T. Kamon,[34] T. Kaneko,[36] K. Karr,[37] H. Kasha,[40] Y. Kato,[24] T. A. Keaffaber,[29] K. Kelley,[19] R. D. Kennedy,[7] R. Kephart,[7] P. Kesten,[18] D. Kestenbaum,[11] H. Keutelian,[7] F. Keyvan,[4] B. Kharadia,[13] B. J. Kim,[30] D. H. Kim,[7a] H. S. Kim,[14] S. B. Kim,[20] S. H. Kim,[36] Y. K. Kim,[18] L. Kirsch,[3] P. Koehn,[23] A. Köngeter,[16] K. Kondo,[36] J. Konigsberg,[8] S. Kopp,[5] K. Kordas,[14] A. Korytov,[8] W. Koska,[7] E. Kovacs,[7a] W. Kowald,[6] M. Krasberg,[20] J. Kroll,[7] M. Kruse,[30] S. E. Kuhlmann,[1] E. Kuns,[32] T. Kuwabara,[36] A. T. Laasanen,[29] S. Lami,[27] S. Lammel,[7] J. I. Lamoureux,[3] M. Lancaster,[18] M. Lanzoni,[27] G. Latino,[27] T. LeCompte,[1] S. Leone,[27] J. D. Lewis,[7] P. Limon,[7] M. Lindgren,[4] T. M. Liss,[13] J. B. Liu,[30] Y. C. Liu,[33] N. Lockyer,[26] O. Long,[26] C. Loomis,[32] M. Loreti,[25] J. Lu,[34] D. Lucchesi,[27] P. Lukens,[7] S. Lusin,[39] J. Lys,[18] K. Maeshima,[7] A. Maghakian,[31] P. Maksimovic,[19] M. Mangano,[27] M. Mariotti,[25] J. P. Marriner,[7] A. Martin,[40] J. A. J. Matthews,[22] R. Mattingly,[19] P. Mazzanti,[2] P. McIntyre,[34] P. Melese,[31] A. Menzione,[27] E. Meschi,[27] S. Metzler,[26] C. Miao,[20] T. Miao,[7] G. Michail,[11] R. Miller,[21] H. Minato,[36] S. Miscetti,[9] M. Mishina,[17] H. Mitsushio,[36] T. Miyamoto,[36] S. Miyashita,[36] N. Moggi,[27] Y. Morita,[17] A. Mukherjee,[7] T. Muller,[16] P. Murat,[27] S. Murgia,[21] H. Nakada,[36] I. Nakano,[36] C. Nelson,[7] D. Neuberger,[16] C. Newman-Holmes,[7] C.-Y. P. Ngan,[19] M. Ninomiya,[36] L. Nodulman,[1] S. H. Oh,[6] K. E. Ohl,[40] T. Ohmoto,[12] T. Ohsugi,[12] R. Oishi,[36] M. Okabe,[36] T. Okusawa,[24] R. Oliveira,[26] J. Olsen,[39] C. Pagliarone,[27] R. Paoletti,[27] V. Papadimitriou,[35] S. P. Pappas,[40] N. Parashar,[27] S. Park,[7] A. Parri,[9] J. Patrick,[7] G. Pauletta,[27] M. Paulini,[18] A. Perazzo,[27] L. Pescara,[25] M. D. Peters,[18] T. J. Phillips,[6] G. Piacentino,[27] M. Pillai,[30] K. T. Pitts,[7] R. Plunkett,[7] L. Pondrom,[39] J. Proudfoot,[1] F. Ptohos,[11] G. Punzi,[27] K. Ragan,[14] D. Reher,[18] A. Ribon,[25] F. Rimondi,[2] L. Ristori,[27] W. J. Robertson,[6] T. Rodrigo,[27] S. Rolli,[37] J. Romano,[5] L. Rosenson,[19] R. Roser,[13] T. Saab,[14] W. K. Sakumoto,[30] D. Saltzberg,[4] A. Sansoni,[9] L. Santi,[27] H. Sato,[36] P. Schlabach,[7] E. E. Schmidt,[7] M. P. Schmidt,[40] A. Scott,[4] A. Scribano,[27] S. Segler,[7] S. Seidel,[22] Y. Seiya,[36] F. Semeria,[2] G. Sganos,[14] T. Shah,[19] M. D. Shapiro,[18] N. M. Shaw,[29] Q. Shen,[29] P. F. Shepard,[28] M. Shimojima,[36] M. Shochet,[5] J. Siegrist,[18] A. Sill,[35] P. Sinervo,[14] P. Singh,[13] K. Sliwa,[37] C. Smith,[15] F. D. Snider,[15] T. Song,[20] J. Spalding,[7] T. Speer,[10] P. Sphicas,[19] F. Spinella,[27] M. Spiropulu,[11] L. Spiegel,[7] L. Stanco,[25] J. Steele,[39] A. Stefanini,[27] J. Strait,[7] R. Ströhmer,[7a] D. Stuart,[7] G. Sullivan,[5] K. Sumorok,[19] J. Suzuki,[36] T. Takada,[36] T. Takahashi,[24] T. Takano,[36] K. Takikawa,[36] N. Tamura,[12] B. Tannenbaum,[22] F. Tartarelli,[27] W. Taylor,[14] P. K. Teng,[33] Y. Teramoto,[24] S. Tether,[19] D. Theriot,[7] T. L. Thomas,[22] R. Thun,[20] R. Thurman-Keup,[1] M. Timko,[37] P. Tipton,[30]

A. Titov,[31] S. Tkaczyk,[7] D. Toback,[5] K. Tollefson,[30] A. Tollestrup,[7] H. Toyoda,[24] W. Trischuk,[14] J. F. de Troconiz,[11] S. Truitt,[20] J. Tseng,[19] N. Turini,[27] T. Uchida,[36] N. Uemura,[36] F. Ukegawa,[26] G. Unal,[26] J. Valls,[7a] S. C. van den Brink,[28] S. Vejcik, III,[20] G. Velev,[27] R. Vidal,[7] R. Vilar,[7a] M. Vondracek,[13] D. Vucinic,[19] R. G. Wagner,[1] R. L. Wagner,[7] J. Wahl,[5] N. B. Wallace,[27] A. M. Walsh,[32] C. Wang,[6] C. H. Wang,[33] J. Wang,[5] M. J. Wang,[33] Q. F. Wang,[31] A. Warburton,[14] T. Watts,[32] R. Webb,[34] C. Wei,[6] H. Wei,[35] H. Wenzel,[16] W. C. Wester, III,[7] A. B. Wicklund,[1] E. Wicklund,[7] R. Wilkinson,[26] H. H. Williams,[26] P. Wilson,[5] B. L. Winer,[23] D. Winn,[20] D. Wolinski,[20] J. Wolinski,[21] S. Worm,[22] X. Wu,[10] J. Wyss,[25] A. Yagil,[7] W. Yao,[18] K. Yasuoka,[36] Y. Ye,[14] G. P. Yeh,[7] P. Yeh,[33] M. Yin,[6] J. Yoh,[7] C. Yosef,[21] T. Yoshida,[24] D. Yovanovitch,[7] I. Yu,[7] L. Yu,[22] J. C. Yun,[7] A. Zanetti,[27] F. Zetti,[27] L. Zhang,[39] W. Zhang,[26] and S. Zucchelli[2]

(CDF Collaboration)

[1] *Argonne National Laboratory, Argonne, Illinois 60439*
[2] *Istituto Nazionale di Fisica Nucleare, University of Bologna, I-40127 Bologna, Italy*
[3] *Brandeis University, Waltham, Massachusetts 02254*
[4] *University of California at Los Angeles, Los Angeles, California 90024*
[5] *University of Chicago, Chicago, Illinois 60637*
[6] *Duke University, Durham, North Carolina 27708*
[7] *Fermi National Accelerator Laboratory, Batavia, Illinois 60510*
[8] *University of Florida, Gainesville, FL 32611*
[9] *Laboratori Nazionali di Frascati, Istituto Nazionale di Fisica Nucleare, I-00044 Frascati, Italy*
[10] *University of Geneva, CH-1211 Geneva 4, Switzerland*
[11] *Harvard University, Cambridge, Massachusetts 02138*
[12] *Hiroshima University, Higashi-Hiroshima 724, Japan*
[13] *University of Illinois, Urbana, Illinois 61801*
[14] *Institute of Particle Physics, McGill University, Montreal H3A 2T8, and University of Toronto, Toronto M5S 1A7, Canada*
[15] *The Johns Hopkins University, Baltimore, Maryland 21218*
[16] *Institut für Experimentelle Kernphysik, Universität Karlsruhe, 76128 Karlsruhe, Germany*
[17] *National Laboratory for High Energy Physics (KEK), Tsukuba, Ibaraki 315, Japan*
[18] *Ernest Orlando Lawrence Berkeley National Laboratory, Berkeley, California 94720*
[19] *Massachusetts Institute of Technology, Cambridge, Massachusetts 02139*
[20] *University of Michigan, Ann Arbor, Michigan 48109*
[21] *Michigan State University, East Lansing, Michigan 48824*
[22] *University of New Mexico, Albuquerque, New Mexico 87131*
[23] *The Ohio State University, Columbus, OH 43210*
[24] *Osaka City University, Osaka 588, Japan*
[25] *Universita di Padova, Istituto Nazionale di Fisica Nucleare, Sezione di Padova, I-36132 Padova, Italy*
[26] *University of Pennsylvania, Philadelphia, Pennsylvania 19104*
[27] *Istituto Nazionale di Fisica Nucleare, University and Scuola Normale Superiore of Pisa, I-56100 Pisa, Italy*
[28] *University of Pittsburgh, Pittsburgh, Pennsylvania 15260*
[29] *Purdue University, West Lafayette, Indiana 47907*
[30] *University of Rochester, Rochester, New York 14627*
[31] *Rockefeller University, New York, New York 10021*
[32] *Rutgers University, Piscataway, New Jersey 08855*
[33] *Academia Sinica, Taipei, Taiwan 11530, Republic of China*
[34] *Texas A&M University, College Station, Texas 77843*
[35] *Texas Tech University, Lubbock, Texas 79409*
[36] *University of Tsukuba, Tsukuba, Ibaraki 315, Japan*
[37] *Tufts University, Medford, Massachusetts 02155*
[38] *Waseda University, Tokyo 169, Japan*
[39] *University of Wisconsin, Madison, Wisconsin 53706*
[40] *Yale University, New Haven, Connecticut 06520*

We present a study of events with W bosons and hadronic jets produced in $\overline{p}p$ collisions at a center of mass energy of 1.8 TeV. The data consist of 51400 $W^{\pm} \rightarrow e^{\pm}\nu$ decay candidates from 108 pb^{-1} of integrated luminosity collected with the CDF detector at the Tevatron Collider. The cross sections and jet production properties have been measured for $W + \geq 1$ to ≥ 4 jet events. The data are compared to predictions of leading order QCD matrix element calculations with added gluon radiation and simulated parton fragmentation.

14.70.Fm, 12.38.Qk, 13.85.Qk

The production of W bosons in $\overline{p}p$ collisions at the Fermilab Tevatron Collider provides the opportunity to test perturbative QCD predictions at large momentum transfers. Previous analyses have used these data to study W production and decay properties [1–3], diboson (WW, WZ, $W\gamma$) production [4,5], and the pair production of top quarks [6,7]. In this Letter, we present cross section measurements and kinematic properties of direct single W boson production with jets. After W events from top decay are removed, the data are compared to quantum chromodynamics (QCD) predictions of single W + jet production. These comparisons test how well the standard model predicts hadronic production properties of W bosons at the highest center of mass energies studied to date.

This analysis uses 108 pb^{-1} of integrated luminosity collected with the CDF detector [8] from 1992–95. The principal detector elements used for this measurement are the vertex tracking chamber (VTX), the central tracking chamber (CTC), and the calorimeters. The VTX, a wire time-projection chamber, locates interactions along the beam direction. The CTC, a cylindrical drift chamber, measures the momenta of charged particles in the region $|\eta| < 1.1$ [9]. Both tracking detectors are immersed in a 1.4 T magnetic field. The electromagnetic and hadronic calorimeters cover the range $|\eta| < 4.2$ and are used to measure the energies of electrons and jets.

$W^{\pm} \rightarrow e^{\pm}\nu$ decay candidates are identified in events that pass a high transverse energy ($E_T = E\sin\theta$) electron trigger. The event selection requires an isolated [10] electron in the central calorimeter ($|\eta| \leq 1.1$) that has $E_T \geq 20$ GeV and satisfies tight selection criteria [11]. The reconstructed neutrino transverse energy ($\not\!\!E_T$), measured from the imbalance of E_T in the calorimeter, must exceed 30 GeV.

Jets in the W events are clustered using a cone algorithm [12] with radius $\Delta R \equiv \sqrt{\Delta\eta^2 + \Delta\phi^2} = 0.4$. We account for parton energy deposited outside the cone, and correct for energy contaminating the cone from both the underlying event and additional $\overline{p}p$ interactions. We count jets with $E_T \geq 15$ GeV and $|\eta| \leq 2.4$, and reject any events that have a jet within $\Delta R = 0.52$ of an electron. Of 51431 W candidate events, 11144 events have $\geq$1 jet, 2596 have $\geq$2 jets, 580 have $\geq$3 jets, 126 have $\geq$4 jets, and 21 have $\geq$5 jets. These jet multiplicities are subsequently corrected for jets produced in additional $\overline{p}p$ interactions that occur in the same bunch crossing as the W event. There is a 1% probability that an event will have a single extra jet; the probability drops by about a factor of 6 for each additional extra jet.

The systematic uncertainties on jet counting are determined by varying the jet energy by $\pm$5%, the jet $|\eta|$ by $\pm$0.2, the probability of jets from additional $\overline{p}p$ interactions by $^{+100\%}_{-50\%}$, and the correction for energy contamination in the jet cone by $\pm$50% ($\pm$0.5 GeV on average). The combined uncertainty ranges from 10% for the $\geq$1 jet sample to 30% for the $\geq$4 jet sample and dominates the uncertainties in the W + jet cross section measurements.

We measure the cross section for $\overline{p}p \rightarrow W$ production as a function of jet multiplicity n from the number of observed W candidates with $\geq n$ jets (N_n) using the equation

$$\sigma_n \cdot \mathrm{BR} = \sigma_0 \cdot \mathrm{BR} \cdot \frac{N_n - B_n}{\epsilon_n} \cdot \frac{\epsilon_0}{N_0 - B_0} \qquad (1)$$

where ϵ_n is the W detection efficiency, B_n is the estimated background, and BR is the branching ratio for $W^{\pm} \rightarrow e^{\pm}\nu$ decay. For the inclusive cross section times branching ratio ($\sigma_0 \cdot$BR) we use a previous CDF measurement of 2490 $\pm$ 120 pb [13]. This method takes advantage of the cancellation of some systematic uncertainties in the ratios, and gives the most accurate relative W + $\geq n$ jet cross sections.

The estimate of B_n in Eq. (1) includes $Z \rightarrow e^+e^-$, $W \rightarrow \tau\nu$, and direct QCD multijet production. The $Z \rightarrow e^+e^-$ and $W \rightarrow \tau\nu$ contributions are small (3%) and have a negligible effect on the ratios. Multijet contamination is measured with a sample obtained by removing the electron isolation and $\not\!\!E_T$ requirements of the W selection and then extrapolating from the multijet-dominated region into the W signal region. This background ranges from (2.9 $\pm$ 0.9)% for the $\geq$0 jet sample to (27 $\pm$ 11)% for the $\geq$4 jet sample.

In order to isolate direct single W production ($q\overline{q'} \rightarrow W$), B_n also includes standard model predictions of diboson and top quark production. The contribution from WW and WZ production is negligible; however, we include a correction to the jet multiplicity to account for $W\gamma$ events in which the photon is reconstructed as a jet. This is predicted to occur in (0.4 $\pm$ 0.1)% of events. The rate of $W^{\pm} \rightarrow e^{\pm}\nu$ events from standard model $t\overline{t}$ ranges from (0.08 ± 0.02)% for $\geq$0 jet events to (26 ± 5)% for $\geq$4 jet events. The cross sections and kinematic distributions are corrected for these contributions.

The final correction to the number of $W^{\pm} \rightarrow e^{\pm}\nu + \geq n$ jet candidates accounts for the efficiency (ϵ_n in Eq. (1)) of identifying $W^{\pm} \rightarrow e^{\pm}\nu$ decays. The acceptance due to restrictions on the electron E_T, $\not\!\!E_T$, and detector fiducial volume was determined using a leading-order QCD calculation [14] for W + $\geq$1 to $\geq$4 jets. The electron-jet overlap rate is calculated directly from the data by taking $Z \rightarrow e^+e^-$ events and replacing the $Z \rightarrow e^+e^-$ decay with a simulated $W^{\pm} \rightarrow e^{\pm}\nu$ decay, preserving the boson transverse momentum (p_T). The overall efficiency also includes the efficiency of the online trigger and the efficiency of the electron identification. The combined efficiency is (19.6 $\pm$ 0.3)% for $W+ \geq$0 jets and remains nearly constant as a function of the number of jets.

The measured cross sections for single $W^{\pm} \rightarrow e^{\pm}\nu$ + $\geq n$ jet events are listed in Table I and plotted in Fig. 1. Also included in Table I are the ratios σ_n/σ_{n-1}, which

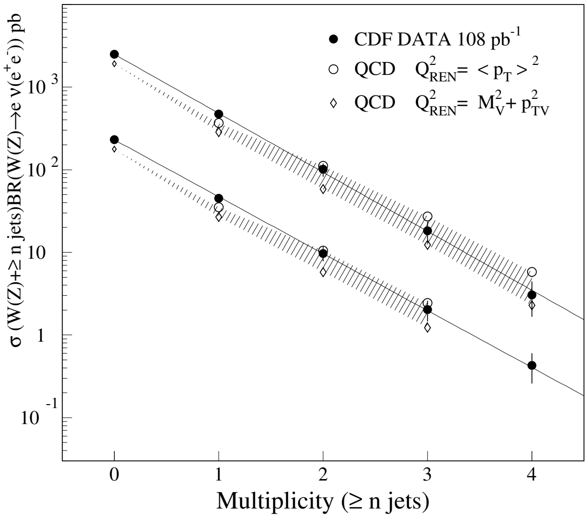

FIG. 1. Cross sections for $W^\pm \to e^\pm\nu + \geq n$ jets (top) and $Z \to e^+e^- + \geq n$ jets (bottom) versus inclusive jet multiplicity. The lines are fits of an exponential to the data. The theory is shown as a shaded band which represents the uncertainty due to the renormalization scale. The ≥ 0 jet prediction is a Born-level calculation for W production.

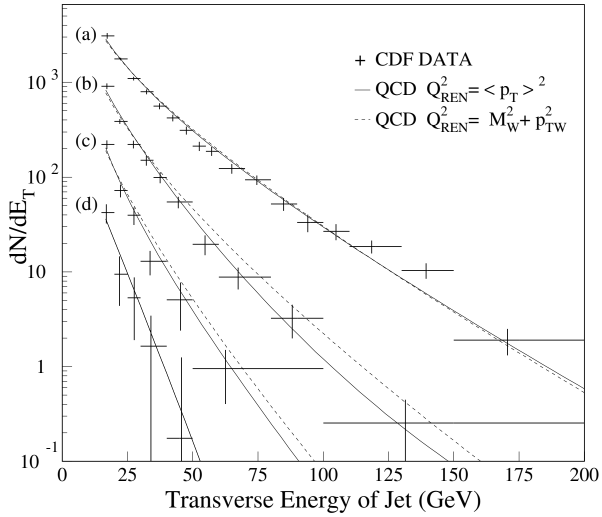

FIG. 2. Transverse energy distribution of the (a) highest E_T jet in ≥ 1 jet events, (b) second highest E_T jet in ≥ 2 jet events, (c) third highest E_T jet in ≥ 3 jet events, and (d) fourth highest E_T jet in ≥ 4 jet events. The curves represent the ELO QCD predictions. The renormalization scale Q^2 is $\langle p_T \rangle^2$ for the solid curves and $M_W^2 + p_{T_W}^2$ for the dashed curves (a–c only). The theory is normalized to the data for each distribution and the errors are the sum of statistical and systematic uncertainties.

show that the cross sections fall by about a factor of five with each additional jet.

The measured cross sections and kinematic distributions are compared to predictions of leading order (LO) pertubative QCD using the VECBOS [14] Monte Carlo program. We use a two-loop α_s evolution evaluated at renormalization scales of either $Q^2 = \langle p_T \rangle^2$ of the partons or $M_W^2 + p_{T_W}^2$ of the boson, representing reasonable extremes. The CTEQ3M [15] parton density functions are used with the factorization scale set to the renormalization scale. The QCD predictions are at least five times more sensitive to the renormalization scale than to the factorization scale or the choice of parton density functions (e.g. MRSA' [16]). Initial state gluon radiation, final state parton fragmentation, and hadronization are simulated using the HERWIG [17] Monte Carlo program. This procedure represents a partial higher-order correction to the tree-level diagrams and we refer to it as enhanced leading order (ELO). The generated hadronic showers are processed with the full CDF detector simulation. The same reconstruction and selection criteria applied to experimental data are used on the simulated data.

The QCD predictions are listed in Table I and plotted with the measured cross sections in Fig. 1. The sensitivity of the calculated cross sections to the renormalization scale is indicated by the shaded band. The harder Q^2 scale ($M_W^2 + p_{T_W}^2$) predicts relative cross sections that are consistent with the measured cross sections but are low in magnitude by about a factor 1.6, while the softer Q^2 scale ($\langle p_T \rangle^2$) predicts cross sections generally closer in magnitude but with a ratio ranging from 1.28 for ≥ 1 jets to 0.53 for ≥ 4 jets. Thus, within the inherent uncertainty of the LO calculation, the predicted and measured $W + \geq n$ jet cross sections are in agreement for $n = 2$ to 4. For comparison, Fig. 1 also shows the cross sections and QCD predictions for $Z + \geq n$ jets from a previous CDF measurement [18]. These have the same general features as W production, but are lower in cross section by about a factor of 10.

Details of the QCD predictions are studied using kinematic distributions of jets in W events. We select events from the ELO simulated W sample with the same selection criteria used for the data. Shape comparisons are made by normalizing the theory to data. We first compare the measured E_T spectra (Fig. 2) of jets 1–4, ordered by decreasing E_T, to the ELO QCD prediction [19]. The sensitivity of the prediction to the renormalization scale is illustrated by varying it from $\langle p_T \rangle^2$ (solid curve) to $M_W^2 + p_{T_W}^2$ (dotted curve). The correspondence between data and theory for these distributions is more clearly seen in Fig. 3, which shows (data–theory)/theory

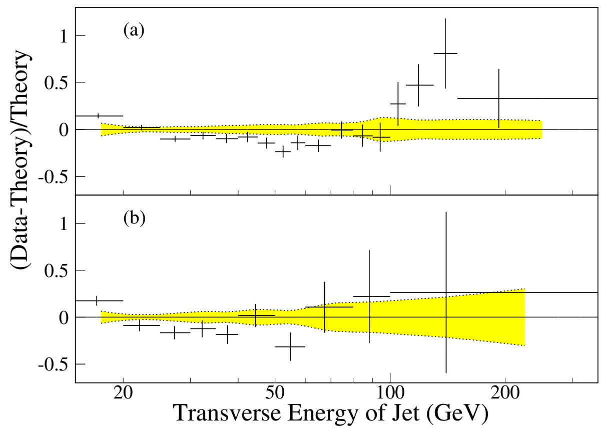

FIG. 3. (Data–theory)/theory ($Q^2 = \langle p_T \rangle^2$) for the jet transverse energy distribution of the first and second highest E_T jets in (a) $\geq$1 and (b) $\geq$2 jet events, respectively. The error bars are statistical uncertainties and the band represents the systematic uncertainty on the shape. The theory is normalized to the data.

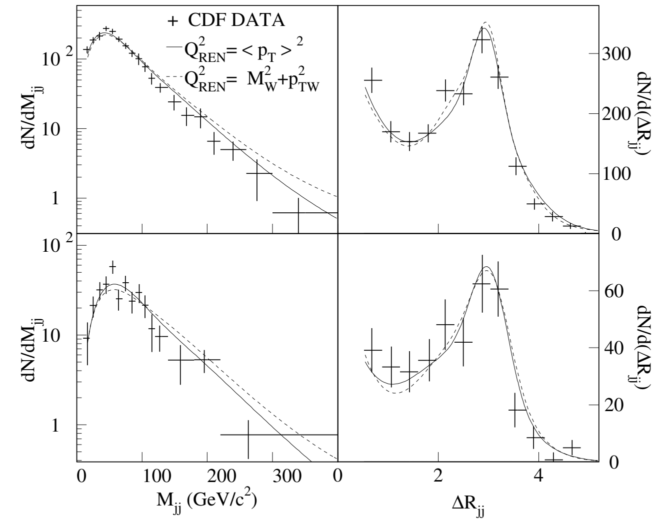

FIG. 4. Distributions of dijet mass and separation in $\eta - \phi$ space between the two highest-E_T jets for W + $\geq$2 jet events (top) and W + $\geq$3 jet events (bottom). The curves represent the ELO QCD predictions: $Q^2 = \langle p_T \rangle^2$ (solid) and $Q^2 = M_W^2 + p_{T_W}^2$ (dashed).

for the same spectra. Correlations between jets are studied by measuring the separation (ΔR_{jj}) and invariant mass (M_{jj}) of pairs of jets. The distributions of ΔR_{jj} and M_{jj} for the two highest E_T jets in $\geq$2 jet and $\geq$3 jet events are shown in Fig. 4. The systematic uncertainties are determined by the change in the distributions when the jet energy and subtracted backgrounds are varied independently within their $\pm 1\sigma$ limits. The error bars in Figs. 2 and 4 include statistical and systematic uncertainties.

The shape comparisons in Figs. 2–4 demonstrate that the ELO QCD predictions reproduce the main features of both the jet E_T and jet-jet correlation distributions. In particular, the measured and predicted jet E_T spectra for the four highest E_T jets generally remain within 15% over three orders of magnitude. The correlation between jets, as measured by ΔR_{jj}, is well predicted by the QCD calculation (Fig. 4c and d), and the measured invariant mass distributions (Fig. 4a and b) are in fair agreement with the QCD predictions. However, the high statistics of our W + $\geq$1 jet sample show the limitation of this QCD prediction. Fig. 3a shows that the theory calculation underestimates the cross section for the lowest E_T (< 20 GeV) and highest E_T (> 100 GeV) jets. These regions rely heavily upon the partial higher-order corrections generated by HERWIG. At low E_T, initial state gluon radiation is sometimes hard enough to become the highest E_T jet and supersede the parton generated in the LO matrix element. For events with the highest jet E_T > 100 GeV, over 50% of the W + $\geq$1 jet events have at least 2 jets which explicitly indicates the need for higher-order corrections to the W + 1 parton calculation. As expected, the ELO QCD calculation only partly corrects for the higher-order QCD terms.

In summary, this Letter contains an analysis of jet production associated with $W^\pm \to e^\pm \nu$ events selected from 108 pb^{-1} of $\overline{p}p$ collisions at a center of mass energy of 1.8 TeV. Data are compared to enhanced LO QCD predictions (LO parton matrix elements with HERWIG-simulated fragmentation) to determine the reliability of QCD calculations. The ratio of the measured to predicted cross section is 1.28 $\pm$ 0.16 ($Q^2 = \langle p_T \rangle^2$) and 1.65 $\pm$ 0.20 ($Q^2 = M_W^2 + p_{T_W}^2$) for $\overline{p}p \to W$ + $\geq$1 jet events. For higher jet multiplicities, the two Q^2 predictions bracket the measurement, with the $Q^2 = M_W^2 + p_{T_W}^2$ prediction at a approximately constant fraction below the measured cross section. The shapes of the QCD-predicted jet production properties are in general agreement with the data, but the statistics of the $W^\pm \to e^\pm \nu$ data are large enough to show some limitations of the enhanced LO QCD predictions.

We thank the Fermilab staff and the technical staffs of the participating institutions for their vital contributions. We also thank Walter Giele and Nigel Glover for many useful discussions. This work was supported by the

n Jets	$\sigma_n \cdot \mathrm{BR}(W^\pm \to e^\pm\nu)$ (pb)	$Q^2 = \langle p_T \rangle^2$ $BR \cdot \sigma_{\mathrm{QCD}}$	$\sigma_{\mathrm{Data}}/\sigma_{\mathrm{QCD}}$	$Q^2 = M_W^2 + p_{T_W}^2$ $BR \cdot \sigma_{\mathrm{QCD}}$	$\sigma_{\mathrm{Data}}/\sigma_{\mathrm{QCD}}$	σ_n/σ_{n-1} (Data)
$\geq$1	471 $\pm$ 5 $\pm$ 57	367 $\pm$ 5	1.28 $\pm$ 0.16	285 $\pm$ 4	1.65 $\pm$ 0.20	0.189 $\pm$ 0.021
$\geq$2	101 $\pm$ 2 $\pm$ 19	112 $\pm$ 5	0.90 $\pm$ 0.17	58.1 $\pm$ 1.5	1.74 $\pm$ 0.33	0.214 $\pm$ 0.015
$\geq$3	18.4 $\pm$ 1.1 $\pm$ 5.2	27.2 $\pm$ 2.1	0.67 $\pm$ 0.20	12.3 $\pm$ 0.6	1.49 $\pm$ 0.44	0.182 $\pm$ 0.020
$\geq$4	3.1 $\pm$ 0.6 $\pm$ 1.3	5.8 $\pm$ 0.7	0.53 $\pm$ 0.25	2.3 $\pm$ 0.2	1.33 $\pm$ 0.62	0.166 $\pm$ 0.042
$\geq$5	0.24 $\pm$ 0.24 $\pm$ 0.28					0.080 $\pm$ 0.109

TABLE I. W + $\geq n$ jet cross sections. The first error on the data cross sections is the statistical error; the second includes the systematic error on the W acceptance, the background systematic, and the jet-counting uncertainty, as described in the text. The QCD Monte Carlo cross sections ($BR \cdot \sigma_{\mathrm{QCD}}$) are generated using VECBOS for Q^2 scales of $\langle p_T \rangle^2$ and $M_W^2 + p_{T_W}^2$. The uncertainties for the theory are statistical.

U.S. Department of Energy and National Science Foundation; the Italian Istituto Nazionale di Fisica Nucleare; the Ministry of Education, Science and Culture of Japan; the Natural Sciences and Engineering Research Council of Canada; the National Science Council of the Republic of China; and the A. P. Sloan Foundation.

[1] F. Abe *et al.*, Phys. Rev. Lett. **76**, 3070 (1996).
[2] F. Abe *et al.*, Phys. Rev. Lett. **70**, 4042 (1993).
[3] S. Abachi *et al.*, Phys. Rev. Lett. **75**, 3226 (1995).
[4] F. Abe *et al.*, Phys. Rev. Lett. **75**, 1017 (1995).
[5] F. Abe *et al.*, Phys. Rev. Lett. **74**, 1936 (1995).
[6] F. Abe *et al.*, Phys. Rev. D **51**, 4623 (1995).
[7] F. Abe *et al.*, Phys. Rev. Lett. **74**, 2626 (1995).
[8] F. Abe *et al.*, Nucl. Instrum. Methods A **271**, 387 (1988).
[9] We use a coordinate system in which z is along the proton direction, ϕ is the azimuthal angle, θ is the polar angle and $\eta \equiv -\ln(\tan\frac{\theta}{2})$ is the pseudorapidity. We take z=0 at the center of the detector for fiducial cuts and at the interaction point for event variables.
[10] An isolated electron is one for which the calorimeter E_T in a cone of radius 0.4 in η–ϕ around the electron cluster is less than 10% of the electron E_T.
[11] F. Abe *et al.*, Phys. Rev. D **44**, 29 (1991), our selection is the same as in this reference except for (i) $0.5 < E/(pc) < 2.0$ and (ii) $\chi^2_{strip} < 10$.
[12] F. Abe *et al.*, Phys. Rev. D **45**, 1448 (1992).
[13] F. Abe *et al.*, Phys. Rev. Lett. **76**, 3070 (1996).
[14] F.A. Berends, W.T. Giele, H. Kuijf, and B. Tausk, Nucl. Phys. **B357**, 32 (1991).
[15] H.L. Lai *et al.*, Phys. Rev. D **51**, 4763 (1995).
[16] A.D. Martin, R.G. Roberts, W.J. Stirling, Phys. Rev. D **51**, 4756 (1995).
[17] G. Marchesini and B. Webber, Nucl. Phys. **B310**, 461 (1988).
[18] F. Abe *et al.*, Phys. Rev. Lett. **77**, 448 (1996).
[19] The curves are fits of analytic functions to the QCD Monte Carlo prediction which accurately reproduce the spectra.